

Microscopic study of the  $\Delta$ -nucleus potential from a many-body Hamiltonian for  $\pi$ ,  $N$ , and  $\Delta$

T. -S. H. Lee

*Argonne National Laboratory, Argonne, Illinois 60439\**  
*and Center for Theoretical Physics, Laboratory for Nuclear Science and Department of Physics,*  
*Massachusetts Institute of Technology, Cambridge, Massachusetts 02139*

K. Ohta<sup>†</sup>

*Center for Theoretical Physics, Laboratory for Nuclear Science and Department of Physics,*  
*Massachusetts Institute of Technology, Cambridge, Massachusetts 02139*

(Received 23 October 1981)

The strength of the  $\Delta$ -nucleus potential is calculated from the many-body Hamiltonian for  $\pi$ ,  $N$ , and  $\Delta$  constructed by Betz and Lee. The results are compared to the empirical values of the  $\Delta$ -hole doorway model. It is found that the calculated strength of the central potential reproduces the empirical one to a large extent. However, the calculated spin-orbit potential is much smaller than that of of the  $\Delta$ -hole model. It is also shown that the pion absorption through the  $N\Delta S$  wave only accounts for about half of the total absorption. The sums of other  $N\Delta$  partial waves are found to be equally important.

[ NUCLEAR REACTIONS A model of interactions between  $\pi$ ,  $N$ , and  $\Delta$  in nuclear matter. Calculation of the  $\Delta$ -nucleus potential. ]

The intermediate pion-nucleus interaction is dominated by  $\Delta$ -isobar excitation inside the nucleus. This motivated the successful isobar-doorway model<sup>1-5</sup> which describes the  $\pi$ -nucleus dynamics in terms of  $\Delta$  propagation in nuclear medium. The  $\Delta$ -hole propagator contains a phenomenological complex spreading potential  $W_{sp}(\vec{r})$  which reflects coupling of the doorway state to more complicated states (e.g., absorption). By a suitable adjustment<sup>3,4</sup> of the strength of  $W_{sp}(\vec{r})$ , the model yielded a satisfactory description of not only the differential cross sections of  $\pi$ -nucleus elastic scattering but also the gross structure of  $\pi$ -nucleus reaction cross sections. However, without a microscopic understanding of the spreading potential  $W_{sp}(\vec{r})$ , the model could not be an internally consistent one for analyzing exten-

sive data of pion-absorption by nuclei. The purpose of this paper is to investigate a microscopic origin of  $W_{sp}(\vec{r})$  based on the many-body Hamiltonian which has recently been constructed by Betz and Lee<sup>6</sup> (BL).

It is necessary here to summarize briefly the content of the BL model. This model can be considered a straightforward extension of the conventional nuclear many-body theory to a higher energy region where real pion production can occur during nuclear collisions. The many-body Hamiltonian of BL is written in terms of three elementary degrees of freedom  $\pi$ ,  $N$ , and  $\Delta$ ,

$$H = H_0 + H_I, \tag{1}$$

where

$$H_0 = \sum_{\tau=\frac{1}{2},\frac{3}{2}} \int d^3p c^\dagger(\vec{p},\tau)[E_\tau(\vec{p})-m]c(\vec{p},\tau) + \int d^3k \alpha^\dagger(\vec{k})\omega(\vec{k})\alpha(\vec{k}), \tag{2}$$

$$H_I = \frac{1}{4} \sum_{\tau'_1\tau'_2\tau_1\tau_2} \int d^3p'_1 d^3p'_2 d^3p_1 d^3p_2 c^\dagger(\vec{p}'_1,\tau'_1)c^\dagger(\vec{p}'_2,\tau'_2)c(\vec{p}_2,\tau_2)c(\vec{p}_1,\tau_1) \langle \vec{p}'_1\tau'_1, \vec{p}'_2\tau'_2 | V_0 | \vec{p}_1\tau_1, \vec{p}_2\tau_2 \rangle$$

$$+ \int d^3k d^3p' d^3p [c^\dagger(\vec{p}',\frac{3}{2})c(\vec{p},\frac{1}{2})\alpha(\vec{k}) \langle \vec{p}',\frac{3}{2} | h | \vec{p},\frac{1}{2}, \vec{k} \rangle + \text{H.c.}]$$

$$+ \int d^3k' d^3p' d^3k d^3p c^\dagger(\vec{p},\frac{1}{2})\alpha^\dagger(\vec{k}')c(\vec{p},\frac{1}{2})\alpha(\vec{k}) \langle \vec{p},\frac{1}{2}, \vec{k}' | v | \vec{p},\frac{1}{2}, \vec{k} \rangle. \tag{3}$$

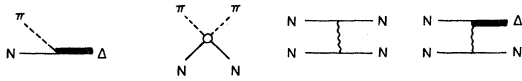


FIG. 1. Basic mechanism of the many-body Hamiltonian of Betz and Lee (Ref. 6).

We dropped all  $z$  components of spin and isospin to abbreviate the presentation. The creation operators for  $\pi$ ,  $N$ , and  $\Delta$  are  $\alpha^\dagger(\vec{k})$ ,  $c^\dagger(\vec{p}, \frac{1}{2})$ , and  $c^\dagger(\vec{p}, \frac{3}{2})$ , respectively. The masses are  $\mu$ ,  $m$ , and  $m_\Delta$  and the energies are  $\omega(k) = (\mu^2 + k^2)^{1/2}$  and  $E_\tau(\vec{p}) = m_\tau + \vec{p}^2/2m_\tau$ . Explicit expressions for the interactions  $h$ ,  $v$ , and  $V_0$  are given by the partial wave expanded forms Eqs. (3.2)–(3.6) and (4.36) in Ref. 6. We depict these interactions in Fig. 1. The  $\Delta\Delta$  and  $N\Delta \Leftrightarrow N\Delta$  parts of  $V_0$  are omitted to simplify the model. Note that the vertex interaction  $h$  describes the  $\pi N P_{33}$  interaction only. Other weaker interactions are represented by the two-body interaction  $v$ . The strategy of the BL model is to determine  $h$ ,  $v$ , and  $V_0$  phenomenologically by fitting the experimental phase shifts of  $\pi N$  scattering up to 300 MeV and  $NN$  scattering up to about 1 GeV, and some available data of  $\pi$ -deuteron reactions. The model is apparently suitable to the study of the  $\Delta$ -nucleus potential.

The  $\Delta$  spreading potential is parametrized<sup>4</sup> as

$$W_{\text{sp}}(\vec{r}) = W_0 f(r) + 2V_{LS}g(r)\vec{S}_\Delta \cdot \vec{L}_\Delta, \quad (4)$$

where  $f(r)$  is assumed to be proportional to the nuclear density,  $g(r)$  is a surface-peaked function,  $\vec{S}_\Delta$  and  $\vec{L}_\Delta$  are, respectively, the spin and orbital angular momenta of  $\Delta$ . Clearly,  $W_{\text{sp}}(\vec{r})$  is only a part of the  $\Delta$ -nucleus potential. Within the framework of the isobar-hole formalism, the  $\Delta$  motion is also influenced by a binding potential and by its decay mechanism  $\Delta \Leftrightarrow \pi N$ . The  $\Delta$ -nucleus potential or the self-energy of  $\Delta$  can be calculated from the  $N\Delta$  Bruckner  $G$  matrix in nuclear matter in a quite similar manner as the  $N$ -nucleus potential is calculated from the  $NN$   $G$  matrix.<sup>7</sup> Our main task is therefore to compute the  $N\Delta$   $G$  matrix in nuclear matter.

It will be helpful to give an insight into the origin

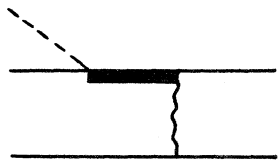


FIG. 2. The simplest absorption mechanism.



FIG. 3. Rescattering corrections to absorption.

of the spreading potential and to mention our essential assumption before going into detail. The most important contribution to the imaginary part of  $W_0$  is absorption. The simplest pion absorption mechanism contained in the BL Hamiltonian is  $\pi NN \Leftrightarrow N\Delta \Leftrightarrow NN$  (Fig. 2). We assume that this mechanism is the dynamical origin of the spreading potential  $W_{\text{sp}}(\vec{r})$ . One might therefore assume that the  $\Delta$  self-energy corresponding to  $W_{\text{sp}}(\vec{r})$  should be the sum of all contributions involving 2 particle-1 hole (2p-1h) intermediate states during  $N\Delta$  collisions in nuclear matter. However, in the BL model 2p-1h states can also be reached via more complicated pion absorption mechanisms as illustrated in Fig. 3. They are characterized by the decay of  $\Delta$  into pion and 1 particle states and subsequent pion rescatterings before reaching 2p-1h states. We do not consider these rescattering effects on absorption.

The above assumption can be stated in mathematical expressions as follows: The starting point is the Dyson equation for the one-particle Green's function  $G(\vec{p}_\Delta, w_\Delta)$  of a  $\Delta$  with momentum  $\vec{p}_\Delta$  and energy  $w_\Delta$  propagating in ordinary nuclear matter,

$$G(\vec{p}_\Delta, w_\Delta) = G_0(\vec{p}_\Delta, w_\Delta) + G_0(\vec{p}_\Delta, w_\Delta) \times \Sigma(\vec{p}_\Delta, w_\Delta) G(\vec{p}_\Delta, w_\Delta), \quad (5)$$

where  $\Sigma(\vec{p}_\Delta, w_\Delta)$  is the sum of all proper self-energy diagrams in the Feynman-Dyson perturbation series.<sup>8</sup> It is then grouped according to the number of nucleon-hole lines in intermediate states of each diagram. We are concerned only with terms in which at most one nucleon is excited above the Fermi sea ( $1h$ -line diagrams). Figure 4 is the only  $0h$  line contribution given by

$$\begin{aligned} \Sigma_{\text{res}}^{(0)}(\vec{p}_\Delta, w_\Delta) &= \int d^3p d^3k \langle \vec{p}_\Delta \frac{3}{2} | h^\dagger | \vec{p} \frac{1}{2}, \vec{k} \rangle \\ &\times \frac{Q_1}{w_\Delta - E_N(\vec{p}) - \omega(\vec{k}) + i\epsilon} \\ &\times \langle \vec{p} \frac{1}{2}, \vec{k} | h | \vec{p}_\Delta \frac{3}{2} \rangle, \quad (6) \end{aligned}$$

where  $Q_1$  is the Pauli operator for the  $\pi N$  intermediate state.

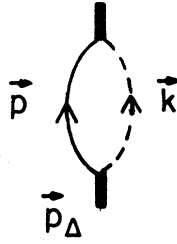


FIG. 4.  $0h$ -line  $\Delta$  self-energy. The nucleon particle and hole lines are, respectively, represented by  $\uparrow$  and  $\downarrow$ .

The  $1h$ -line contributions can be separated into two different parts,

$$\Sigma^{(1)}(\vec{p}_\Delta, w_\Delta) = \Sigma_{\text{abs}}^{(1)}(\vec{p}_\Delta, w_\Delta) + \Sigma_{\text{res}}^{(1)}(\vec{p}_\Delta, w_\Delta). \quad (7)$$

$\Sigma_{\text{abs}}^{(1)}(\vec{p}_\Delta, w_\Delta)$  is the sum of all the graphs in which the external  $\Delta$  lines couple directly to  $2p$ - $1h$  states through the interaction  $V_0$ . Some examples of these graphs are shown in Fig. 5. These are contributions from the direct absorption mechanism indicated in Fig. 2. No  $\Delta \rightleftharpoons \pi N$  vertex interactions act on the initial or final  $\Delta$ . All other graphs in which at least one of the external  $\Delta$  lines decays through the  $\Delta \rightleftharpoons \pi N$  interaction are summarized as  $\Sigma_{\text{res}}^{(1)}(\vec{p}_\Delta, w_\Delta)$  and some of them are illustrated in Fig. 6. From its definition  $\Sigma_{\text{res}}^{(1)}(\vec{p}_\Delta, w_\Delta)$  can be considered higher order terms of the simplest self-energy Eq. (6) and can be renormalized into the latter. Indeed all of these rescattering diagrams can be cast in the  $1h$  line contributions to the renormalization effects on the  $\Delta \rightleftharpoons \pi N$  vertex, excepting Figs. 6(a) and (b) which are nucleon and pion propagator renormalizations. In particular, all the contributions to the  $\Delta$  self-energy coming from absorption as described by Fig. 3 are  $\Delta \rightleftharpoons \pi N$  vertex corrections. One sees that the absorption mechanism of Fig. 3 is mixed with the direct absorption Fig. 2 to make up the vertex correction diagram Fig. 6(c).

It is seen above that the  $\Delta$  self-energy contains two distinctive dynamics; rescattering and absorp-

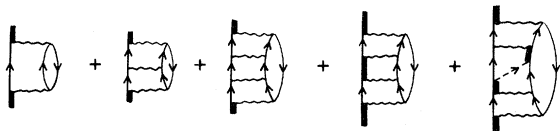


FIG. 5.  $1h$ -line  $\Delta$  self-energy coming from the sum of all the interactions between two nucleon particles in the  $2p$ - $1h$  states sandwiched by  $V_0$ .

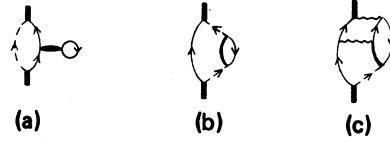


FIG. 6.  $1h$ -line  $\Delta$  rescattering diagrams which are renormalization corrections to the  $0h$ -line diagram Fig. 4. The blob in (a) is for the  $NN$   $G$  matrix defined by Eq. (10d).

tion. We calculate each of them to lowest order in hole-line expansion, namely, rescattering to  $\Sigma_{\text{res}}^{(0)}(\vec{p}_\Delta, w_\Delta)$  and absorption to  $\Sigma_{\text{abs}}^{(1)}(\vec{p}_\Delta, w_\Delta)$ . Inclusion of  $\Sigma_{\text{res}}^{(1)}(\vec{p}_\Delta, w_\Delta)$  does not necessarily produce an improvement upon  $\Sigma_{\text{res}}^{(0)}(\vec{p}_\Delta, w_\Delta)$ . If we include  $\Sigma_{\text{res}}^{(1)}(\vec{p}_\Delta, w_\Delta)$ , it introduces modifications of the  $\Delta \rightleftharpoons \pi N$  vertex so that the isobar-hole interaction  $W$  as well as the Pauli blocking term  $\delta W$  of  $\Sigma_{\text{res}}^{(0)}(\vec{p}_\Delta, w_\Delta)$  must also be modified. To be consistent with the analyses<sup>3,4</sup> using the simplest one-pion exchange isobar-hole interaction  $W + \delta W$ , it seems reasonable to neglect  $\Sigma_{\text{res}}^{(1)}(\vec{p}_\Delta, w_\Delta)$ . The nucleon propagator renormalization term Fig. 6(a) contributes chiefly to the real part of the  $\Delta$  binding potential. We also ignore this effect (we will discuss this term later).

The  $1h$ -line absorption self-energy as defined above can be written as

$$\Sigma_{\text{abs}}^{(1)}(\vec{p}_\Delta, w_\Delta) = \int_{p < p_F} d^3p \langle \vec{p}_\Delta \frac{3}{2}, \vec{p} \frac{1}{2} | G(w = w_\Delta + \epsilon_N(\vec{p})) | \vec{p}_\Delta \frac{3}{2}, \vec{p} \frac{1}{2} \rangle. \quad (8)$$

$G(w)$  is the sum of all interactions between two baryons sandwiched by  $V_0$ . The summation is performed above the Fermi sea applying Bruckner's method. The resulting equation for  $G(w)$  in the two-baryon subspace  $NN \oplus N\Delta$  is

$$G(w) = V_0 + V_0 \frac{Q_2}{w - H_0 - V_D(w)} G(w) + V_0 \frac{Q_2}{w - H_0 - V_D(w)} G_c(w) \times \frac{Q_2}{w - H_0 - V_D(w)} G(w) \quad (9a)$$

with

$$G_c(w) = \tilde{V}_c(w) + \tilde{V}_c(w) \frac{Q_2}{w - H_0 - V_D(w)} G_c(w), \quad (9b)$$

$$\tilde{V}_c(w) = V_E(w) + V_B(w). \quad (9c)$$

Here  $Q_2$  is the Pauli operator of the subspace  $NN \oplus N\Delta$  and the effective  $N\Delta$  interactions  $V_D(w)$ ,  $V_E(w)$ , and  $V_B(w)$  are, respectively, defined as

$$V_D(w) = \sum_i h_i^\dagger \frac{Q_3}{w - H_0} h_i, \quad (10a)$$

$$V_E(w) = \sum_{i \neq j} h_i^\dagger \frac{Q_3}{w - H_0} h_j, \quad (10b)$$

$$V_B(w) = \sum_i h_i^\dagger \frac{Q_3}{w - H_0} G_{NN}(w) \frac{Q_3}{w - H_0} h_i, \quad (10c)$$

where  $h_i$  stands for the  $\Delta \rightleftharpoons \pi N$  vertex of the  $i$ th baryon.  $Q_3$  is the Pauli operator for  $\pi NN$  intermediate states and  $G_{NN}(w)$  is the  $NN$   $G$  matrix calculated in the presence of a spectator pion,

$$G_{NN}(w) = V_0 + V_0 \frac{Q_3}{w - H_0} G_{NN}(w). \quad (10d)$$

The effective interactions  $V_D(w)$ ,  $V_E(w)$ , and  $V_B(w)$  are shown by the diagrams in Fig. 7. Within the

BL model, it is found that the effect of  $V_B(w)$  is small except in the  $N\Delta$   $S$  wave. Furthermore,  $V_B(w)$  is the interaction appearing in calculating the graph Fig. 6(a) in  $\Sigma_{\text{res}}^{(1)}(\vec{p}_\Delta, w_\Delta)$ . We drop this interaction for evaluation of  $G(w)$  in accordance with the neglect of  $\Sigma_{\text{res}}^{(1)}(\vec{p}_\Delta, w_\Delta)$ .

The structure of Eqs. (9) and (10) is identical with that of the coupled two-baryon scattering equation in Ref. 6 [see its Eqs. (4.11) and (4.18)], the only difference being the presence of the Pauli operators. The angular-averaged Pauli operators<sup>9</sup> are used in our calculation. Then the numerical method of Ref. 6 can be used to solve the  $G$  matrix equation in the partial wave representation. No details will therefore be given here except to note that the  $G$  matrix depends on the total momentum of the two baryons as well as the starting energy.

Following the current practice,<sup>7</sup> we calculate the central part of  $W_{\text{sp}}(\vec{r})$  from the  $1h$ -line absorption self-energy in infinite nuclear matter as  $W_0 = \Sigma_{\text{abs}}^{(1)}(\vec{p}_\Delta, w_\Delta)$ . In terms of the partial wave expanded  $G$  matrix (using the convention of Ref. 6),  $W_0$  as a function of  $p_\Delta$  is written as

$$W_0(p_\Delta) = (2\pi)^3 \frac{3}{4\pi p_F^3} \rho_0 \sum_{L_\Delta S_\Delta J T} \frac{(2J+1)(2T+1)}{64} \frac{1}{4\pi} \int_{p < p_F} d^3p G_{L_\Delta S_\Delta, L_\Delta S_\Delta}^{JT}(q, q; W(\vec{p}_\Delta, \vec{p})), \quad (11)$$

where

$$q = \left| \frac{m_\Delta \vec{p} - m \vec{p}_\Delta}{m + m_\Delta} \right|, \quad (12)$$

$$W(\vec{p}_\Delta, \vec{p}) = \epsilon_N(\vec{p}) + \epsilon_\Delta(\vec{p}_\Delta) - \frac{(\vec{p} + \vec{p}_\Delta)^2}{2(m + m_\Delta)}. \quad (13)$$

For an arbitrary choice of  $f(r)$  in Eq. (4),  $\rho_0$  is given by

$$\rho_0 = A/4\pi \int_0^\infty r^2 dr f(r). \quad (14)$$

If  $f(r)$  is taken to be the standard Woods-Saxon form,  $\rho_0$  corresponds to the density of nuclear matter with the Fermi momentum  $p_F$ . The single particle energies of  $N$  and  $\Delta$  are specified as follows: Following the standard nuclear matter theory,<sup>10</sup> we choose

$$\begin{aligned} \epsilon_N(\vec{p}) &= m + \frac{\vec{p}^2}{2m^*} + U_0, \quad p \leq p_F, \\ &= m + \frac{\vec{p}^2}{2m}, \quad p > p_F. \end{aligned} \quad (15)$$

The  $\Delta$ -single particle energy is determined self-consistently<sup>7</sup>

$$\epsilon_\Delta(\vec{p}_\Delta) = m_\Delta + \frac{\vec{p}_\Delta^2}{2m_\Delta} + \text{Re} \left[ \Sigma(\vec{p}_\Delta, \epsilon_\Delta(\vec{p}_\Delta)) \right]. \quad (16a)$$

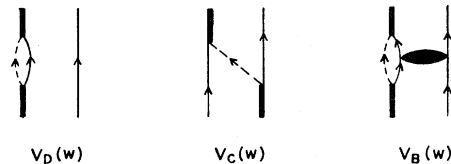


FIG. 7. Effective  $N\Delta$  interactions defined by Eqs. (10a)–(10c).

Note that the total  $\Delta$  self-energy

$$\Sigma(\vec{p}_\Delta, w_\Delta) = \Sigma_{\text{res}}^{(0)}(\vec{p}_\Delta, w_\Delta) + \Sigma_{\text{abs}}^{(1)}(\vec{p}_\Delta, w_\Delta) \quad (16b)$$

enters into the self-consistent equation (16a).

In order to determine the strength of the spin-

$$V_{LS}(p_\Delta) = (2\pi)^3 \frac{3}{4\pi p_F^3} \frac{\rho_0}{20r_0^2 p_\Delta^2} \sum_{L_\Delta S_\Delta J T} \frac{(2J+1)(2T+1)}{64} \frac{S_\Delta(S_\Delta+1)+3}{S_\Delta(S_\Delta+1)} [J(J+1) - L_\Delta(L_\Delta+1) - S_\Delta(S_\Delta+1)] \\ \times \frac{1}{4\pi} \int_{p < p_F} d^3p \frac{\vec{p}_\Delta \cdot \vec{q}}{q^2} G_{L_\Delta S_\Delta, L_\Delta S_\Delta}^{JT}(q, q; W(\vec{p}_\Delta, \vec{p})), \quad (17a)$$

with

$$g(r) = \frac{r_0^2}{r} \frac{d}{dr} f(r). \quad (17b)$$

$r_0$  is any constant length to make  $g(r)$  dimensionless.

The spreading potential thus obtained is dependent on the  $\Delta$  momentum  $p_\Delta$ , namely, it is nonlocal. To compare with the phenomenological local potential determined by Horikawa, Thies, and Lenz,<sup>4</sup> we must construct an equivalent local potential. As Negele and Yazaki<sup>12</sup> have recently pointed out, the nonlocality of the optical potential influences the equivalent local potential. However, since the resulting  $W_0$  is not a rapidly varying function of  $p_\Delta$  in the relevant momentum region  $p_\Delta \leq 400$  MeV/c, we do not consider effects of the nonlocality here but obtain a local potential by choosing the incident pion momentum

$$k_\pi = [(E_\pi + \mu)^2 - \mu^2]^{1/2}$$

as an average value of  $p_\Delta$  ( $E_\pi$  is the pion kinetic energy).

The parameters used in the calculation are  $\rho_0 = 0.17$  fm<sup>-3</sup>,  $p_F = 1.36$  fm<sup>-1</sup>,  $r_0 = 1.1$  fm,  $U_0 = -80$  MeV, and  $m^* = 0.68 m$ . The results of  $W_0(p_\Delta)$  and  $V_{LS}(p_\Delta)$  are shown in Figs. 8 and 9. Only the imaginary part of  $W_0$  can be directly compared to that of the isobar-hole model.<sup>4</sup> Comparison of other parts of the potential can meaningfully be made only in the shape-independent quantities

$$\Omega = \frac{4\pi}{A-1} \int_0^\infty r^2 dr W_0 f(r) \\ = \frac{A}{A-1} \frac{W_0}{\rho_0}, \quad (18)$$

orbit potential, we must derive the  $\Delta$  self-energy  $\Sigma(\vec{p}'_\Delta, \vec{p}_\Delta; w_\Delta)$  in finite nuclei and extract a term proportional to  $\vec{S}_\Delta \cdot \vec{p}'_\Delta \times \vec{p}_\Delta$ . If we assume that the momentum transfer  $\vec{p}'_\Delta - \vec{p}_\Delta$  caused by the nuclear density variation near the nuclear surface is small, it is straightforward to express the spin-orbit strength in terms of  $G(w)$  using a Thomas-Fermi type approximation.<sup>11</sup> The result is

$$S = \int_0^\infty r dr V_{LS} g(r) \\ = -V_{LS} r_0^2 f(0), \quad (19)$$

where  $f(0) = 1$ . These are shown in Figs. 10 and 11.

From Fig. 8 it is seen that the calculated strength of  $\text{Im}W_0$  agrees qualitatively with the phenomenological one.<sup>4</sup> Theoretical values amount to about 85% of the empirical ones on the average. As shown in Refs. 3 and 4, the imaginary spreading potential can account for the measured total pion-absorption cross section. The agreement obtained here indicates that the dominant absorption

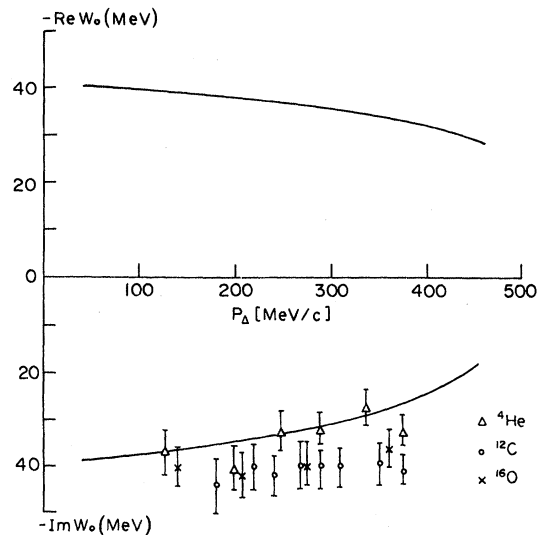


FIG. 8. Strength of the  $\Delta$  central potential,  $W_0(p_\Delta)$ . The empirical values are taken from Ref. 4 by estimating the  $\Delta$  momentum  $p_\Delta$  from the pion momentum  $k_\pi$ .

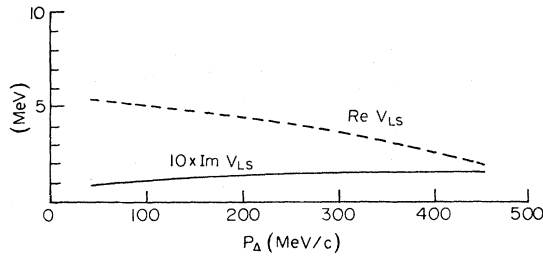


FIG. 9. Strength of the  $\Delta$  spin-orbit potential,  $V_{LS}(p_{\Delta})$ .

mechanism must be the process shown in Fig. 2. This interpretation must be carefully distinguished from that of many-nucleon absorption implied essentially by a kinematic analysis of inclusive pion absorption data.<sup>13</sup> There involves a nontrivial and model-dependent problem of separating initial and final state interactions from the absorption mechanism. The only way to clarify the situation seems to be to study the consequences of the BL Hamiltonian (1)–(3) using the two-nucleon absorption approach of this work and to analyze the data of Ref. 13 and others. The research in this direction will be discussed elsewhere.

The calculated  $\Omega$  for  $^{12}\text{C}$  and  $^{16}\text{O}$  (Fig. 10) agrees qualitatively with that of Ref. 4. The discrepancy for  $^4\text{He}$  is significant but the use of the  $G$  matrix in nuclear matter and the local density approximation for such a light nucleus is very questionable. It is

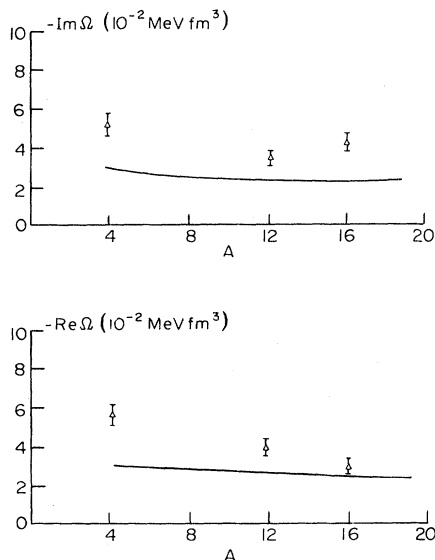


FIG. 10. Volume integral  $\Omega$  of the  $\Delta$  central potential. The empirical values are taken from Ref. 4.

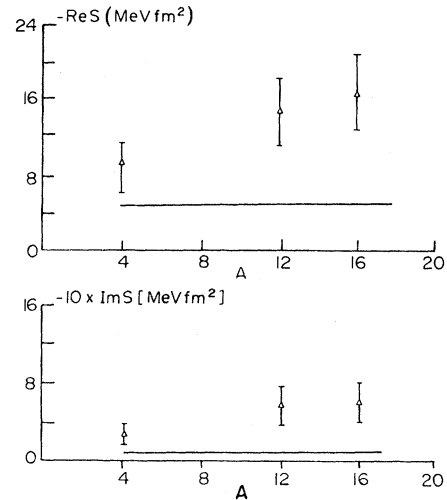


FIG. 11. Surface integral  $S$  of the  $\Delta$  spin-orbit potential strength function. The empirical values are taken from Ref. 4.

important to note that in our calculation the real part of  $\Omega$  comes from the  $1h$ -line absorption diagram, while that of Ref. 4 also includes the contribution from a real  $\Delta$  binding potential. It would seem that the  $1h$ -line absorption contains the most important physics of the central part of the  $\Delta$ -nucleus potential.

Contrary to this, the calculated  $S$  for the spin-orbit interaction (Fig. 11) is much smaller than the empirical values. According to Ref. 4, the  $\Delta$ -nucleus spin-orbit interaction is roughly the same as the nucleon-nucleus spin-orbit interaction. Our result  $2V_{LS} \approx 8$  MeV at  $p_{\Delta} = 262$  MeV/c is less than half of the  $N$ -nucleus spin-orbit strength  $\approx 17$  MeV (Ref. 14). The phenomenological procedure for extracting the spin-orbit interaction suffers from larger uncertainties (see discussions in Ref. 4) and the discrepancy we have found will not easily be resolved until the freedom of the analyses is reduced by imposing additional constraints. Of course approximations we have made might be incorrect for calculating the spin-orbit interaction. The neglect of Fig. 6(a) could be partially responsible for the disagreements. The second-order diagrams with respect to the  $G$  matrix can also be sources of the  $\Delta$  spin-orbit coupling as in the nucleon case.<sup>15</sup> The origin of the nucleon-nucleus spin-orbit force is one of the most fundamental and important problems in nuclear physics but is most poorly understood. Much work will have to be done for the consistent understanding of both of the  $N$ - and  $\Delta$ -spin-orbit interactions.

TABLE I. Contributions of important partial waves to  $W_0$  and  $W_{LS}$  at  $p_\Delta = 261.74$  MeV/c.

$N\Delta$	Channels $NN$	$\text{Re}W_0$ (MeV)	$\text{Im}W_0$ (MeV)	$\text{Re}V_{LS}$ (MeV)	$\text{Im}V_{LS}$ (MeV)
$^5S_2$	$^1D_2$	-3.28	-18.30	0	0
$^3P_0$	$^3P_0$	-8.20	-2.30	2.13	0.59
$^3P_1 + ^5P_1$	$^3P_1$	-4.86	-0.66	1.01	0.14
$^3P_2 + ^5P_2$	$^3P_2 + ^3F_2$	-11.18	-5.14	-0.19	0.03
$^5P_3$	$^3F_3$	-4.17	-4.74	-0.66	-0.74
$^5D_0$	$^1S_0$	-4.36	-0.76	2.05	0.35
$^5D_4$	$^1G_4$	-0.72	-0.73	-0.23	-0.23
	Total	-36.76	-32.62	4.12	0.14

To examine the absorption mechanism in more detail, we present in Table I the contributions of important  $N\Delta$  partial waves to  $W_0$  and  $V_{LS}$ . An essential point emerges here. Although the  $N\Delta$  partial wave  $^5S_2$  is the biggest contribution (-18.30 MeV) to  $\text{Im}W_0$ , the sum of other partial waves (-14.30 MeV) is of the same magnitude. This result is somewhat unexpected but is actually not surprising because the inelasticities of the  $NN$  partial waves listed in Table I are not small (see Fig. 3 of Ref. 6). Our results indicate the importance of treating absorption consistently with the two-nucleon data. Although some geometrical factors favor absorption through the  $N\Delta$   $^5S_2$  wave, calculations of absorption must be carried out with a careful treatment of all partial waves. Equal weight of all partial waves are also clearly exhibited in their contributions to  $\text{Re}W_0$  and  $V_{LS}$  shown in Table I.

We have provided a microscopic picture of the

phenomenological spreading potential  $W_{sp}(\vec{r})$  entering the isobar-hole model. We should mention here that the isobar-hole model<sup>3,4</sup> can rigorously be formulated from the BL many-body Hamiltonian. In this sense the BL model furnishes us with an internally consistent description of  $\pi$ -nucleus interaction *with the  $\pi N$  and  $NN$  data as inputs to the model*. It is hoped that in the future the  $\pi$ -nucleus data can be understood in a deeper theoretical approach by combining the ideas behind the construction of the isobar-hole model and the many-body Hamiltonian.

We would like to thank E. Moniz for many helpful discussions. One of us (T.-S.H.L.) would like to thank A. Kerman for his kind hospitality at the Center for Theoretical Physics, MIT. This work was supported in part through funds provided by the U. S. Department of Energy (DOE) under Contract DE-AC02-76ER03069.

\*Permanent address.

†On leave of absence from University of Tokyo, Tokyo, Japan.

<sup>1</sup>L. S. Kisslinger and W. L. Wang, Phys. Rev. Lett. **30**, 1071 (1973); Ann. Phys. (N.Y.) **99**, 374 (1976).

<sup>2</sup>M. Hirata, F. Lenz, and K. Yazaki, Ann. Phys. (N.Y.) **108**, 116 (1977).

<sup>3</sup>M. Hirata, J. H. Koch, F. Lenz, and E. J. Moniz, Ann. Phys. (N.Y.) **120**, 205 (1979).

<sup>4</sup>Y. Horikawa, M. Thies, and F. Lenz, Nucl. Phys. **A345**, 386 (1980).

<sup>5</sup>W. Weise, Nucl. Phys. **A278**, 402 (1977); E. Oset and W. Weise, *ibid.* **329**, 365 (1979).

<sup>6</sup>M. Betz and T.-S. H. Lee, Phys. Rev. C **23**, 375 (1981).

<sup>7</sup>J. R. Jeukenne, A. Lejeune, and C. Mahaux, Phys. Rep. **25**, 83 (1976); J. S. Bell and E. J. Squires, Phys. Rev. Lett. **3**, 96 (1959).

<sup>8</sup>A. Fetter and J. D. Walecka, *Quantum Theory of Many-particle Systems* (McGraw-Hill, New York, 1971). The standard field-theoretical method is directly applicable to our calculation of the  $\Delta$  self-energy. With finite range form factors, the model is free of divergences.

<sup>9</sup>B. Day and F. Coester, Phys. Rev. C **13**, 1720 (1976).

<sup>10</sup>B. Day, Rev. Mod. Phys. **50**, 495 (1978).

<sup>11</sup>R. R. Scheerbaum, Phys. Lett. **61B**, 151 (1976).

<sup>12</sup>J. W. Negele and K. Yazaki, Phys. Rev. Lett. **47**, 71 (1981); S. Fanton, B. L. Friman, and V. R. Pandharipande, Phys. Lett. **104B**, 89 (1981).

<sup>13</sup>R. D. McKeon *et al.*, Phys. Rev. Lett. **44**, 1033 (1980).

<sup>14</sup>A. Bohr and B. R. Mottelson, *Nuclear Structure* (Benjamin, New York, 1975), Vol. 1.

<sup>15</sup>K. Ohta, T. Terasawa, and M. Tohyama, Phys. Rev. C **22**, 2233 (1980).